ARKIV FÖR FYSIK Band 14 nr 18

Communicated 10 September 1958 by Ivar Waller and Kai Siegbahn

Interactions in flight of negative heavy mesons

By S. Nilsson and Å. Frisk

With 4 figures in the text

ABSTRACT

41 m of K^- track length have been followed in the energy interval 0–140 MeV. 208 interactions in flight are analysed to yield the total cross section per nucleus in emulsion $\sigma = 780 \pm 60$ mb. The corresponding average total nucleon cross section in nuclear matter is calculated to be $\bar{\sigma} = 80 \pm 15$ mb. The mean free path $\lambda = 0.95 \times 10^{-13}$ cm implies a large absorptive potential ~ 60 MeV. The derived limits on the free neutron cross sections do not contradict the assumption that charge independence holds in the absorption and scattering processes. The differential cross section for elastic scattering between 5°–30° is given. An attractive K^- nuclear potential is inferred from the percentage of re-emerging K^--mesons.

1. Introduction

The beams of machine produced positive and negative heavy mesons have made it possible to study their interaction properties in flight. The first experiments [1, 2, 3] showed the quite different behaviour of the K-particles of opposite charge. The positive K-particle has simple interaction properties, which have been studied in a number of experiments (4). The interaction properties of the negative K-particle are on the contrary very complicated due to the many possible reaction channels [5, 6].

The free proton and neutron reactions are most conveniently studied in hydrogen and deuterium bubble chambers. The emulsion technique furnishes information on interactions with complex nuclei and on interactions with free protons in emulsion.

The present paper concerns interactions in flight of negative K-mesons in emulsion. The main emphasis is laid on the possibility to derive the mean free path of the K^- in nuclear matter and accordingly to get information about the cross section on neutrons, which up till now is completely unknown. Deuterium bubble chamber experiments are, however, in progress [8]. In Part 2 and 3 the experimental details and the details of the interactions in flight are presented. In Part 4 the free proton events are reported. In Part 5 the cross sections in emulsion and nuclear matter are derived. Part 6 reports the inelastic scattering events and the escape probability is calculated. Part 7 concerns the differential cross section for elastic scattering.

2. Experimental details

The present experiment was carried out in two Ilford G5 emulsion stacks. Stack 1 (4″×7″, 600 μm, 60 pellicles) was exposed to the partly separated 400 MeV/c K^- beam at the Bevatron and Stack 2 (4″×7″, 600 μm, 32 pellicles) to the separated 300 MeV/c beam.

Tracks with suitable ionisation were picked up in an unbiased way and followed until they came to rest, interacted or left the stacks. In this way 41 m of K^- track length have been followed, 10 m in the energy interval 0–140 MeV (Stack 1) and 31 m in the interval 0–90 MeV (Stack 2). The track length distribution is shown in Table 1.

Table 1. Track length distribution.

Energy MeV	Track length mm	Energy MeV	Track length mm
0–10	723	70– 80	6 226
10–20	1752	80– 90	3 816
20–30	2655	90–100	1 495
30–40	3646	100–110	1 293
40–50	4670	110–120	1 382
50–60	5678	120–130	1 070
60–70	6354	130–140	497
			Total: 41 257

In the high energy stack all tracks which gave rise to an interaction or left the stack were identified by $g^* - p\beta$ measurements. This was necessary as the percentage of background tracks of the right ionisation was high (49 % K^-, 28 % π, 23 % p). In the low energy stack scattering measurements on a sample of 60 showed that most of the tracks were due to K^--mesons (98 % K^-, 2 % π and p) as was also born out by the tracks followed to rest. Consequently all tracks with ionisation and range in agreement with those of a K^--meson were taken as K^--mesons.

The energy of an interacting meson was determined as the weighted mean of the estimates from residual range, g^* and in many cases $p\beta$. Account was taken of the momentum spread across the plate when the residual range was calculated from the known mean range in the stack. The momentum spread was appreciable, 2 MeV/c per cm, in stack 2.

All scatterings with projected angle $\geqslant 2°$ were recorded in stack 2.

A total of 1124 K^- were followed. 818 interacted at rest and 208 interacted in flight with a kinetic energy of the $K^- \geqslant 10$ MeV. All secondary prongs have been followed. The experimental information has been conveniently collected on a punch card system.

3. Characteristics of interactions in flight

The details of the interactions in flight are given in Table 2. Only events with $T_{K^-} \geqslant 10$ MeV were considered in order to exclude contamination from events at rest.

Table 2. Characteristics of the interactions in flight.

Type of interaction	No.
A. Events with at least 1 baryon prong $\geq 5\ \mu$m	151
B. Events with 1 min. prong or π and blob $< 5\ \mu$m or electron	4
C. Events with 1 min. prong or light meson only	20
D. Zero prong events with blob or electron	3
E. Zero prong events with clean end	19
F. $K^- +$ free $p \rightarrow K^- + p$	3
G. $K^- +$ free $p \rightarrow \Sigma + \pi$	2
H. K^- reemerges with energy loss	3
I. τ^-	3

The groups A, B, D, and H are due to interactions with complex nuclei. An investigation [9] of the probable decays C shows that ~ 4 events are interactions and the rest compatible with decays. Some of the zero prong events might be decays in flight where the secondary is not seen. We estimate the fraction of lost π-mesons in this case as $\sim 5\ \%$. Further some of the zero prong stars might be $K^- +$ free proton charge exchange scatterings or absorptions giving only neutral particles. The effects of interactions in group C, free proton events and events with lost pions in group E tend to cancel each other. Thus the numbers in A, B, D, E, and H are a fairly unbiased estimate of the number of K^- interactions with complex nuclei in emulsion.

The number of interactions in each energy interval is given in Table 3.

Table 3. Number of K^- interactions in flight per 10 MeV.

Energy interval	No. of events	Energy interval	No. of events
10–20	8	70– 80	22
20–30	19	80– 90	13
30–40	22	90–100	3
40–50	20	100–110	6
50–60	32	110–120	8
60–70	22	120–140	5

The mean kinetic energy of the K^--meson is $\langle T_{K^-} \rangle = 60$ MeV.

4. Free proton events and K^-–p cross sections

3 $K^- +$ free proton elastic scattering and 2 $K^- +$ free proton absorption events were found. In order to be interpreted as free proton events they had to fulfill the three criteria; coplanarity, energy balance and momentum balance. In the case of the elastic scatterings they could be stringently applied. The kinetic energy of the incoming K^- and the scattering angle in the C.M.S. are given in Table 4. All two prong events were checked in order to see if they could be K^--free p collisions.

In the absorption events the Σ-hyperon decayed in flight and consequently the energy and momentum conservation could be applied less stringently. The

Table 4. K^- + free p elastic scatterings.

T_K, MeV	Scattering angle in C.M.S.
27	48.6°
58	57.9°
63	45.5°

Table 5. K^- + free $p \to \Sigma + \pi$.

T_K, MeV	Angle between the π and the K in C.M.S.	The hyperon decay
68	98°	$\Sigma \to \pi$ i. f.
70	122°	$\Sigma \to \pi$ i. f.

Σ energy was determined by carefully calibrated ionisation measurements, which were used in a separate investigation of hyperon events at rest and will be reported elsewhere [10]. There are no doubt about the identification as free proton events. The data are summarized in Table 5.

In the following analysis the values of the elastic and total absorption cross section will be needed. We take as best estimates from emulsion data at $\langle T_{K^-} \rangle = 60$ MeV [11, 26]:

$$\sigma^{\mathrm{el}}_{K^-p} = 50 \pm 5 \text{ mb},$$
$$\sigma^{a}_{K^-p}(\Sigma^+ + \Sigma^-) = 15 \pm 4 \text{ mb}.$$

The elastic cross section is energy independent in the energy region concerned and constant in the $\cos\theta$ distribution in the C.M.S. There has been disagreement between the emulsion and bubble chamber data [7] on the absorption cross section. The bubble chamber data refers to low energies and the explanation for the discrepancy is probably that the absorption cross section increases rapidly at low energies. This is also indicated by some emulsion experiments [12].

The above absorption cross section refers to production of charged Σ-hyperons. We shall need the total absorption cross section. The bubble chamber experiments give the production rates in hydrogen $\Sigma^- : \Sigma^+ : \Sigma^0 = 2:1:1$ [7]. Further the Λ^0 production rate is probably less than half of the Σ^0 rate. The contribution to the total absorption cross section from Λ^0 production can thus be neglected and the total absorption cross section

$$\sigma^{a}_{K^-p}(\Sigma^+ + \Sigma^- + \Sigma^0) = 20 \pm 5 \text{ mb}$$

will be used.

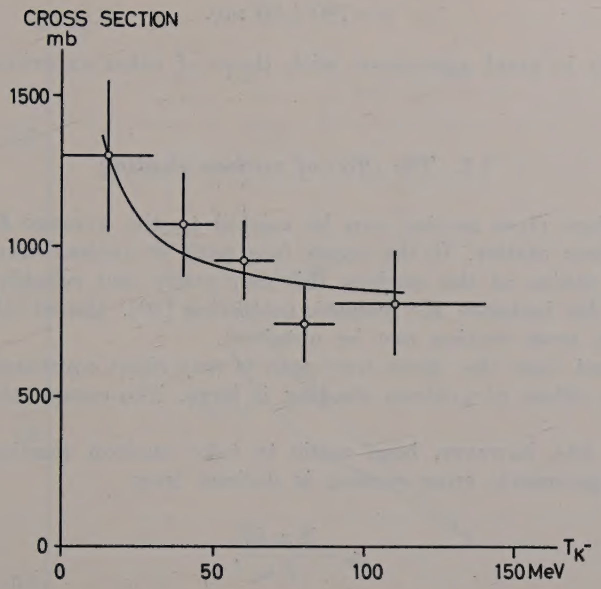

Fig. 1. Cross section per nucleus in emulsion as a function of the K^- kinetic energy. The solid line shows the relation $\sigma' = 780\ (1 + 10/T_{K^-})$.

5. Cross sections in emulsion and nuclear matter

5.1 *Total cross section in emulsion*

The mean free path for absorption and inelastic scattering in emulsion can be obtained from the figures in Tables 1 and 3. The mean free path λ is converted to cross section per nucleus by means of the relation

$$\sigma\,(\mathrm{mb}) = \frac{213}{\lambda\,(m)}.$$

The total cross section as a function of energy is shown in Fig. 1. The increase at low energies is consistent with that expected from the Coulomb attraction effect [13]

$$\sigma' = \sigma\,(1 + V_c/T_{K^-}),$$

where σ' is the measured cross section, σ the true nuclear cross section and V_c the Coulomb potential. The least square fit

$$\sigma' = 780\ (1 + 10/T_{K^-})$$

is also shown in Fig. 1.

The true total nuclear cross section is thus largely energy independent in the energy region 15–110 MeV with a magnitude

$$\sigma = 780 \pm 60 \text{ mb}.$$

This result is in good agreement with those of other experiments (14, 15, 16, 17, 18, 19).

5.2. *The effect of nucleon shading*

The K^--nucleus cross section can be related to the average K^--nucleon cross section in nuclear matter. If the mean free path in nuclear matter is long compared to the radius of the nucleus this can easily and reliably be done. This is the case in for instance K^+ inelastic scattering [20]. Useful information about the K^+-neutron cross section can be obtained.

In the present case the mean free path is very short compared to the nuclear radius and the effect of nucleon shading is large. The computational difficulties also increase.

An attempt has, however, been made to take nucleon shading into account.

An average geometric cross section is defined from

$$\sigma_0 = \frac{\Sigma n_i R_i^2}{\Sigma n_i}, \tag{1}$$

where the sum runs over all elements in emulsion (C, N, O, Br, Ag) except hydrogen.

n_i = the number of atoms/cm³.
$R = r_0 A^{\frac{1}{3}}\, 10^{-13}$ cm = the radius of the nucleus.

The value $r_0 = 1.2$ has been chosen.

The latest data on emulsion composition [12] give $\sigma_0 = 550$ mb with a corresponding geometric mean free path in emulsion of $\lambda_0 = 39$ cm (hydrogen excluded).

The calculations are made for the corresponding mean nucleus with $R = 4.18 \times 10^{-13}$ cm and mass number $A = 43$. This implies that 26 % of the interactions occurs in light nuclei and 74 % in heavy nuclei.

The general expression for the reaction cross section is [22]

$$\sigma = 2\pi R^2 \int_0^{1+r} b\,(1 - e^{-\varkappa A})\, d b, \tag{2}$$

where b = the impact parameter in units of R
r = the interaction radius defined from $\bar{\sigma} = \pi r^2 R^2$
$\varkappa$ = the fraction of the nuclear volume cut out by a cylinder with cross section $\bar{\sigma}$ at a distance b from the centre of the nucleus to the axis of the cylinder.
$\bar{\sigma}$ = the average K^--nucleon cross section defined by

$$\bar{\sigma} = \tfrac{1}{2}\,(\sigma_{K^-p} + \sigma_{K^-n}). \tag{3}$$

σ_{K^-p}, σ_{K^-n} are the free K^--nucleon cross sections and equal numbers of protons and neutrons are assumed.

$\bar{\sigma}$ is related to the mean free path λ in nuclear matter by the relation

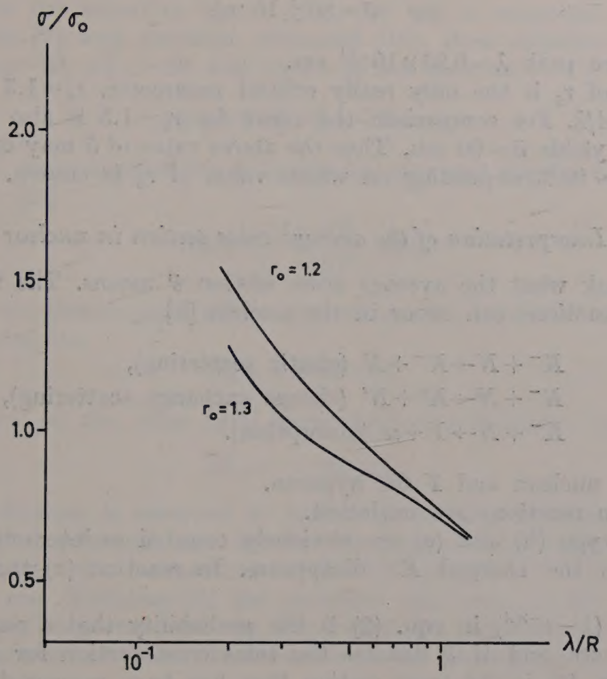

Fig. 2. The relation between the cross section per nucleus in emulsion and the mean free path in nuclear matter.

$$\bar{\sigma}\ (\text{mb}) = \frac{73}{\lambda\ (\text{in units of } 10^{-13}\ \text{cm})}, \quad r_0 = 1.2. \tag{4}$$

Equation (2) can be solved by repeated numerical integrations. In order to facilitate the calculations the fraction $\varkappa$ was approximated (Appendix I) by

$$\left.\begin{aligned} \varkappa &= \frac{3}{2\pi}\, r \left\{\sin^{-1} u_+ - \sin^{-1} u_- + u_+ \sqrt{1-u_+^2} - u_- \sqrt{1-u_-^2}\right\} \quad \text{for } b < 1 - r, \\ \varkappa &= \frac{3}{2\pi}\, r \left\{\frac{\pi}{2} - \sin^{-1} u_- - u_- \sqrt{1-u_-^2}\right\} \quad \text{for } b > 1 - r; \\ & u_\pm = b \pm r, \qquad \bar{\sigma} = 4\, r^2 R^2, \\ & b \text{ and } r \text{ in units of } R. \end{aligned}\right\} \tag{5}$$

The approximation is good to a few per cent.

The integral was then computed numerically for different values of $\bar{\sigma}$. The result is shown in Fig. 2, where σ/σ_0 is given as a function of λ/R. One notices that edge effects become more important as σ increases and the curve cannot safely be extrapolated to obtain the mean free path of for instance antiprotons. At $\bar{\sigma} = 100$ mb about $\frac{1}{3}$ of the contribution to σ comes from regions outside the nuclear surface.

The value $\sigma/\sigma_0 = 780/550$ implies

$$\bar{\sigma} = 80 \pm 15 \text{ mb}$$

or a mean free path $\lambda = 0.95 \times 10^{-13}$ cm.

The value of r_0 is the only really critical parameter. $r_0 = 1.3$ implies $\sigma_0 = 650$ mb and $\bar{\sigma} = 94/\lambda$. For comparison the curve for $r_0 = 1.3$ is also given in Fig. 2. Thus $r_0 = 1.3$ yields $\bar{\sigma} = 90$ mb. Thus the above value of $\bar{\sigma}$ may contain a systematic error of ~ 10 % depending on which value of r_0 is chosen.

5.3. *Interpretation of the average cross section in nuclear matter*

One may ask what the average cross section $\bar{\sigma}$ means. The following strong one-nucleon reactions can occur in the nucleus [5]

$$K^- + N \rightarrow K^- + N \text{ (elastic scattering)}, \tag{6 a}$$

$$K^- + N \rightarrow K^0 + N' \text{ (charge exchange scattering)}, \tag{6 b}$$

$$K^- + N \rightarrow Y + \pi \text{ (absorption)}. \tag{6 c}$$

N stands for nucleon and Y for hyperon.

Two-nucleon reactions are neglected.

Events of type (b) and (c) are obviously counted as interactions in the sense of Sect. 3 as the charged K^- disappears. In reaction (a) the K^- retains its identity.

The factor $(1 - e^{-\varkappa A})$ in equ. (2) is the probability that a reaction with cross section $\bar{\sigma}$ occurs and if $\bar{\sigma}$ denotes the total cross section for all processes (6) then σ in equ. (2) is the cross section that has been measured in emulsion.

The fate of the particles after the first interaction only influences the relative rates of the processes (6), measured outside the nucleus.

Thus the deduced average cross section is interpreted as the total average cross section in nuclear matter.

$$\bar{\sigma} = \bar{\sigma}^a + (\bar{\sigma}^{\text{el}} + \bar{\sigma}^{\text{c.e.}})\, f(T). \tag{7}$$

a denotes absorption, el. elastic scattering and c.e. charge exchange scattering.

The factor $f(T)$ is due to the Pauli Principle. There is one nucleon in the final state for the reactions (a) and (b) and as all states below the maximum Fermi momentum are occupied small momentum transfers and correspondingly the free nucleon cross sections will be suppressed. It is given explicitly in the paper by B. Bhowmik *et al.* [20] for K-N collisions.

The absorption cross section is not affected as there is no nucleon in the final state.

Of the quantities in (7) $\bar{\sigma}$, $\sigma^{a}_{K^- p}$ and $\sigma^{\text{el}}_{K^- p}$ are known, $\sigma^{\text{c.e.}}_{K^- p}$ is known approximately and the neutron cross sections are completely unknown.

5.4. *The relation between the free neutron cross sections*

The factor $f(T) = 0.75$ for $\langle T_{K^-} \rangle = 60$ MeV and a maximim Fermi momentum $p_F = 215$ MeV/c. The additional Coulomb potential energy has been taken into account but no K^--nuclear potential is included. An attractive potential would increase the value of $f(T)$, a repulsive potential would decrease it. $f(T)$ is, however, not very sensitive to changes in energy.

If we assume the tentative figure $\sigma^{\text{c.e.}}_{K^-p} \sim 50$ mb as suggested by the bubble chamber results [7] and emulsion estimates [16], then equation (7) gives with $\bar{\sigma} = 80$ mb, $\sigma^{a}_{K^-p} = 20$, $\sigma^{\text{el}}_{K^-p} = 50$ and $\sigma^{\text{c.e.}}_{K^-p} = 50$ mb inserted

$$\sigma^{a}_{K^-n} + 0.75\,\sigma^{\text{el}}_{K^-n} \sim 75 \text{ mb}. \tag{8}$$

The neutron cross sections for a particular spin and angular momentum state are related by [25]

$$\sigma^{\text{el}}_{K^-n} = \frac{|1-\eta|^2}{(1-|\eta|^2)}\,\sigma^{a}_{K^-n},$$

where η is a complex number. $\sigma^{\text{el}}_{K^-n} = \sigma^{a}_{K^-n}$ when $\sigma^{a}_{K^-n}$ attains its maximum value. Equ. (8) then implies

$$\sigma^{a}_{K^-n} < \sim 45 \text{ mb}.$$

Scattering can on the other hand occur without absorption and from (8)

$$\sigma^{\text{el}}_{K^-n} < \sim 100 \text{ mb}.$$

If charge indepence is assumed to hold in the absorption and scattering processes some useful relations can be derived from isobaric spin considerations. Using the isobaric spin assignment of $T = 1/2$ proposed for the K-particle by Gell-Mann [5] and Nishijima [6] the processes can occur in the $T = 0$ and the $T = 1$ states for the proton and the $T = 0$ state for the neutron [23, 24]. If only one angular momentum state contributes to the absorption at these energies,

$$\sigma^{a}_{K^-n} \leqslant 2\,\sigma^{a}_{K^-p} \sim 40 \text{ mb}.$$

The same relation is true for the scattering process

$$\sigma^{\text{el}}_{K^-n} \leqslant 2\,\sigma^{\text{el+c.e.}}_{K^-p} \sim 200 \text{ mb}.$$

The two deduced upper limits do not contradict the conditions imposed if the forces of the reactions are assumed to be charge independent.

6. Inelastic scattering events. Indication of an attractive K^--nuclear potential

6.1. *Inelastic scattering events*

The kinetic energy of the incoming K^-, the relative energy loss and the scattering angle in the lab. system are given in table 6 for the three events, where the K^- re-emerges.

Table 6. Events with re-emerging K^-.

T_K, MeV	Relative energy loss $\Delta T/T$	Scattering angle (lab. syst.)	Interpreted as
64	0.360	91°	inelastic scatt.
64	0.828	35°	,,
34	0.780	73°	,,

In all cases the K^- made a star of $\geqslant 2$ prongs at rest. All secondary prongs making a star with one or more prongs have been identified as π-mesons, Σ-hyperons or K^--mesons. If the re-emerging K^- made a zero prong star it would not have been observed. Consequently the number has to be corrected by the percentage of K_ϱ^- at rest which is 15 % in our case. A small correction for geometrical bias is also included because 3.2 % of the prongs of appropriate ionisation leave the stacks.

Finally one arrives at the percentage of re-emerging $K^- = 2 \pm 1$ %. Various experiments report a figure between $1-4$ % [26].

6.2. *The probability of escape*

The percentage of inelastically scattered K^- has now to be compared with the escape probability expected from the mean free path in nuclear matter, $\lambda/R = 0.22$, and the branching ratio of the elastic cross section to the total cross section.

One way is to do a Monte Carlo calculation. This has been done by W. Alles *et al.* [16]. The method has the advantage that the distribution of the relative energy losses for various assumed K^--nuclear potentials also comes out from the calculation.

We have calculated the probability to escape from a geometrical picture. The particle will on an average travel a distance λ in the nucleus before it interacts. At the interaction a fraction $\nu = \bar{\sigma}^{\mathrm{el}}/\bar{\sigma}^{\mathrm{tot}}$ will be elastically scattered. If one draws a sphere with radius λ around the point with impact parameter b at a distance λ from the nuclear surface the particles scattered into the solid angle subtended by the intersection of the sphere and the nucleus will reach the nuclear surface without a second interaction. Assuming that all particles reaching the nuclear surface after the first scattering will escape, that the angular distribution at the interaction point is isotropic and that no particles scattered twice or more will escape, the escape probability can be written (Appendix II)

$$P_e = \tfrac{1}{2}\nu\left\{1 - 2\int_0^1 db\, b\cos\left(\mathrm{tn}^{-1}\frac{b}{\sqrt{1-b^2}-\lambda}\right)\right\}; \tag{9}$$

b and λ in units of R.

The angular distribution of the scattered particles is not isotropic in the lab. system due to the movement of the center of momentum. This will result in less particles reaching the considered solid angle. This tendency is compensated for by the fact that some particles scattered more then once will re-emerge. The calculation is valid only for a K^--nuclear potential $= 0$ because in case of an attractive potential K^--particles of low energies will be trapped. Another point is that the K^- kinetic energy after the scattering must exceed the Coulomb potential energy. This is generally the case for a K^- with $T_{K^-} = 60$ MeV.

The result is for $\lambda/R = 0.22$, $P_e = 8$ %, 12 % and 17 % for $\nu = \frac{1}{3}$, $\frac{1}{2}$ and $\frac{2}{3}$ respectively. The values of ν cover all reasonable possibilities. The result of Sect. 5.2 gives $\nu = 0.63$. The figures are in very good agreement with the Monte Carlo calculation for $V_R = 0$ [16] (8 %, 12 % and 21 % respectively).

Thus the percentage of re-emerging K^- is in contradiction with the expected probability of escape for the measured mean free path by a factor three or more if some mechanism does not prevent the K^- from leaving the nucleus. The simplest explanation is to assume an attractive real K^--nuclear potential.

7. Elastic scattering

7.1. *Small angle scattering*

All elastic scatterings with plane angle $\geqslant 2^\circ$ were recorded in stack 2. There was an experimental bias in picking up angles 2°–3° and in the final analysis only plane angles $\geqslant 4^\circ$ and space angles $\geqslant 5^\circ$ were used. We believe that the space angle distribution is unbiased for angles $\geqslant 5^\circ$.

196 single scatterings with space angles 5°–30° were obtained in the energy interval 20–80 MeV. The elasticity was investigated by comparing the range distribution of events with and without single scatterings. No difference was found. The cross section for elastic scattering in barns/ster. as a function of the midpoint of the angular interval is shown in Fig. 3. The experimental cross section is corrected for the loss of events by imposing the plane angle cut off of 4°. In Fig. 3 the expected Coulomb scattering is also shown using an extended charge for the nucleus. It is taken from ref. [28] and shifted according to the difference in mean energy.

The scattering of a particle by a nucleus may be described by an optical model [27] assuming a scattering potential of the type

$$V_{KN} = V_c + V_R + i\,V_I.$$

The imaginary part of the potential is approximately

$$V_I = \hbar\sqrt{\frac{T_{K^-}}{2\,m_{K^-}}}\cdot\frac{1}{\lambda}$$

T_{K^-} = the kinetic energy of the K^- in the nucleus which implies $V_I \sim 60$ MeV for $\lambda = 0.95\times 10^{-13}$ cm and $T_{K^-} \sim 70$ MeV.

The imaginary potential is large, probably larger than the real part of the potential. This means that it is impossible to infer the magnitude of the real potential from observation of interference effects in the differential cross section. The enhanced cross section over the Coulomb cross section indicates an attractive real potential in agreement with the result of the previous section but nothing can be said about its magnitude.

In previous attempts to interpret the elastic cross section [28, 29] a small imaginary potential has been assumed.

7.2. *Large angle scattering*

7 cases of large angle elastic scattering $> 30^\circ$ were found in the energy region $10 - 140$ MeV. The energy loss was zero within the limits of measurements in each case. In particular no "slightly inelastic" events of the type frequently occurring in K^+ scattering were found. The kinetic energy of the incoming K^- and the scattering angle in the lab. system are given in Table 7.

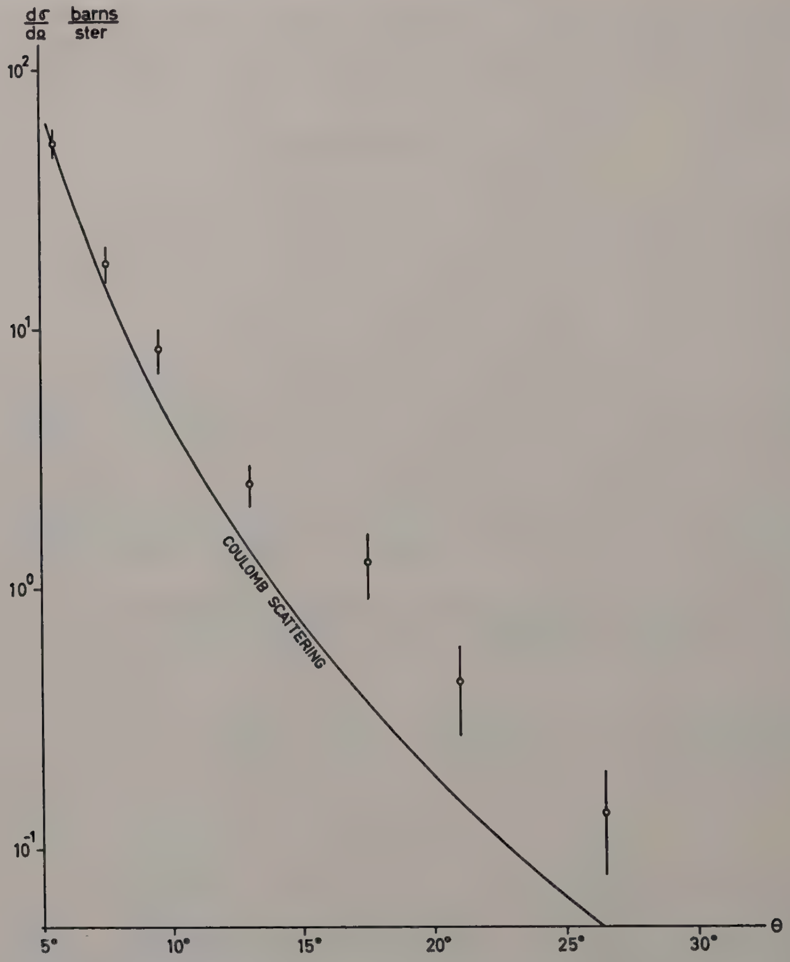

Fig 3. Differential cross section for elastic scattering 5°–30°. $\langle T_{K^-}\rangle = 47$ MeV.

Table 7. Large angle elastic scattering events.

T_{K^-}, MeV	Scattering angle (lab. syst.)
19	33°
25	32°
84	33°
47	33°
22	45°
85	40°
31	90°

The last two events had recoils 2.1 μm and 3.3 μm respectively in the direction of the transferred momentum. The momentum transfer was 206 MeV/c and 254 MeV/c respectively. The ranges in emulsion of a nitrogen nucleus [30] of the corresponding momenta are 2.1 μm and 3.1 μm. The energy transfer will be ~2–3 MeV, which cannot be detected by direct measurements. The events are interpreted as $K^- + (\mathrm{C, N, O})$ elastic scattering.

The above events have been seen in a track length of 40.2 m. The cross section for large angle elastic scattering is accordingly

$$\sigma = 82 \pm 30 \text{ mb/ster. at } \langle\theta\rangle = 44^\circ \text{ and } \langle T_{K^-}\rangle = 45 \text{ MeV}.$$

8. Conclusions

The present experiment permits the following conclusions:

(i) The total average cross section per nucleus in emulsion is energy independent in the energy region 15 – 110 MeV with a magnitude

$$\sigma = 780 \pm 60 \text{ mb}.$$

(ii) The effect of nucleon shading is calculated. Taking this into account the mean free path of the negative K-meson in nuclear matter is

$$\lambda = 0.95 \times 10^{-13} \text{ cm}$$

when the nuclear radius $R = 1.2 \times A^{\frac{1}{3}} \times 10^{-13}$ cm is chosen. This implies a large absorptive potential of about 60 MeV. The corresponding average total nucleon cross section is

$$\bar{\sigma} = 80 \pm 15 \text{ mb}.$$

(iii) The free neutron elastic cross section is less than ~45 mb and the absorption cross section less than ~100 mb, if the processes are assumed to be dominated by one angular momentum state at a mean kinetic energy of the K^- of 60 MeV.

(iv) The above upper limits do not contradict the upper limits imposed by the requirement of charge independence.

(v) The K^- re-emerges in 2 ± 1 % of the interactions. The calculated probability of escape for the measured mean free path and zero nuclear potential is ~10 %. The discrepancy is taken as an indication of an attractive real K^--nuclear potential, which traps the K^- in the nucleus.

(vi) The cross section for elastic scattering 5°–30° is given. Due to the large imaginary potential no conclusions can be drawn from this distribution as regards the magnitude of the real part of an assumed potential.

(vii) The cross section for elastic large angle scattering 30°–90° is

$$\sigma = 82 \pm 30 \text{ mb/ster.}$$

at the mean point $\langle\theta\rangle = 44^\circ$ $\langle T_{K^-}\rangle = 45$ MeV.

ACKNOWLEDGEMENTS

We would like to thank Professor E. J. Lofgren for his kind cooperation, Professor G. Goldhaber and Dr. G. Ekspong for exposing and members of the Bristol and Berkeley groups for processing the stacks. We are grateful to our team of scanners: Mrs. I. Nilsson, Miss I. Durén, Mrs. S. Eklund, Miss V. Braun and Miss B. Lundqvist. We thank Dr. G. Ekspong for many illuminating discussions and valuable advice. We would like to thank Professor K. Siegbahn for his support and encouragement of this work.

This work is partly sponsored by the Air Research and Development Command through its European office, which is gratefully acknowledged. We are indebted to the Swedish Atomic Energy Commission for financial support.

Institute of Physics, University of Uppsala, Uppsala, Sweden

APPENDIX I

The fraction of a sphere cut out by a cylinder

The problem is to find a convenient expression for the fraction $\varkappa$ cut out of sphere with radius R by a cylinder with radius r at a distance b from the centre of the sphere. The cross-sectional area of the cylinder is $\bar{\sigma}=\pi r^2$. The cross-section of the cylinder is substituted by a rectangle with sides $2r$ and r defined by $\bar{\sigma}=4r^2$. The volume of the parallelepiped can then be written approximately

$$V=4\,r\int_{b-r}^{b+r}\sqrt{R^2-x^2}\,dx;$$

x = the distance from the centre of a circle with radius R to a point between $b-r$ and $b+r$ which for the fraction $\varkappa$ gives

$$\varkappa=\frac{3}{2\pi}\,r\left\{\sin^{-1}u_+-\sin^{-1}u_-+u_+\sqrt{1-u_+^2}-u_-\sqrt{1-u_-^2}\right\}\quad b<1-r,$$

b and r in units of R,

and

$$\varkappa=\frac{3}{2\pi}\,r\left\{\frac{\pi}{2}-\sin^{-1}u_--u_-\sqrt{1-u_-^2}\right\}\quad b>1-r,$$

$$u_\pm=b\pm r.$$

APPENDIX II

Calculation of the probability of escape

The notation is given in Fig. 4. The angle θ_0 is given by

$$\theta_0=\operatorname{tn}^{-1}\frac{b}{\sqrt{R^2-b^2-\lambda}}.$$

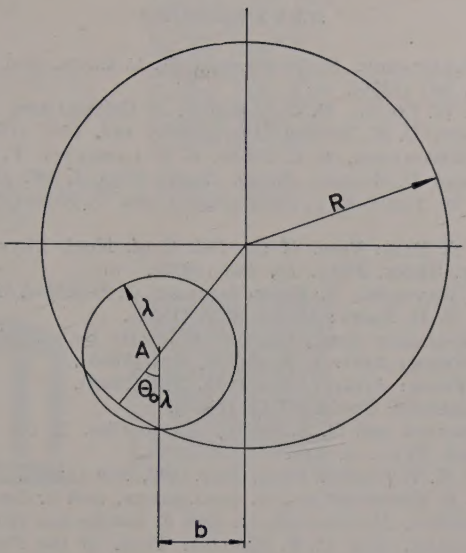

Fig. 4. Figure to Appendix II.

The fraction of particles between b and $b+db$ is

$$\frac{2\pi\, b\, db}{\pi R^2}.$$

The fraction of elastically scattered particles at the point A is

$$\nu = \frac{\bar{\sigma}^{\mathrm{el}}}{\bar{\sigma}^{\mathrm{el}} + \bar{\sigma}^{\mathrm{c.e.}} + \bar{\sigma}^{a}}.$$

The fraction scattered into the solid angle between 0 and θ_0 is

$$\int_0^{\theta_0} \tfrac{1}{2} \sin \theta \, d\theta$$

if the particles are emitted isotropically.

Thus the fraction reaching the surface cut out by the intersection of a sphere with radius λ around the point A and the sphere with radius R is

$$P_e = \tfrac{1}{2}\nu \left\{ 1 - 2\int_0^1 db\, b \cos\left(\mathrm{tn}^{-1} \frac{b}{\sqrt{1-b^2-\lambda}} \right) \right\}$$

with b and λ in units of R.

P_e is an estimate of the escape probability as discussed in the text.

REFERENCES

1. W. W. Chupp, G. Goldhaber, S. Goldhaber, E. L. Iloff, and J. E. Lannutti: Suppl. Nuovo Cim. *4*, 361 (1956).
2. J. E. Lannutti, W. W. Chupp, G. Goldhaber, S. Goldhaber, E. Helmy, E. L. Iloff, A. Pevsner, and D. M. Ritson: Phys. Rev. *101*, 1617 (1956).
3. G. Goldhaber, S. Goldhaber, E. L. Iloff, J. E. Lannutti, F. H. Webb, M. Widgoff, A. Pevsner, and D. Ritson: Suppl. Nuovo Cim. *4*, 367 (1956).
4. A compilation can be found in C. Franzinetti and G. Morpurgo: Suppl. Nuovo Cim. *6*, 469 (1957).
5. M. Gell-Mann and A. Pais: Proc. of the Int. Conf. Nucl. Phys., Glasgow (1954).
6. K. Nishijima: Progr. Theor. Phys. *13*, 285 (1955).
7. L. W. Alvarez, H. Bradner, P. Falk-Vairant, J. D. Gow, A. H. Rosenfeld, F. T. Solmitz, and R. D. Tripp: UCRL-3775 (1957).
8. Proc. of the VIII Rochester Conf., Genève (1958): to be published.
9. S. Nilsson and Å. Frisk: Arkiv f. Fysik 14, 293 (1958).
10. S. Nilsson and Å. Frisk: Arkiv f. Fysik 14, 303 (1958).
11. Proc. of the VII Rochester Conf.: VI-13 (1957).
12. R. G. Glaser, N. Seeman and G. A. Snow; Nuovo Cim. *7*, 142 (1958).
13. A. E. S. Green: Nucl. Phys., p. 234.
14. D. M. Fournet and M. Widgoff: Phys. Rev. *102*, 929 (1956).
15. F. Webb, E. Iloff, F. Fetherstone, G. Goldhaber, and S. Goldhaber, unpublished.
16. W. Alles, N. N. Biswas, M. Ceccarelli, and J. Crussard: Nuovo Cim. *6*, 571 (1957).
17. T. F. Hoang, A. Engler, and M. F. Kaplon: Proc. of the Padua-Venezia Conf., II-48 (1957).
18. W. H. Barkas, W. F. Dudziak, P. C. Giles, H. H. Heckman, F. W. Inman, C. J. Mason, N. A. Nichols, and F. M. Smith: Phys. Rev. *105*, 1417 (1957).
19. E. Lohrmann, M. Nicolić, M. Schneeberger, P. Waloschek, and H. Winzeler: Nuovo Cim. *7*, 163 (1958).
20. B. Bhowmik, D. Evans, S. Nilsson, D. J. Prowse, F. Anderson, D. Keefe, A. Kernan, and J. Losty: Nuovo Cim. *6*, 440 (1957).
21. A. J. Svinnerton and C. Waller: Data from Ilford Research Laboratories (1957).
22. B. Rossi: High Energy Particles, p. 359.
23. S. Gasiorowicz; UCRL-3074 (1955).
24. T. Kotani: UCRL-3072 (1957).
25. I. M. Blatt and V. F. Weisskopf: Theor. Nucl. Phys. p. 321.
26. Summary by G. Goldhaber: Proc. of the Padua-Venezia Conf., XIX-8 (1957).
27. S. Fernbach, R. Serber, and T. B. Taylor: Phys. Rev. *75*, 1352 (1949).
28. B. Bhowmik, D. Evans, D. Falla, G. N. Fowler, A. A. Kamal, and D. J. Prowse: Proc. of the Padua-Venezia Conf., II-45 (1957).
29. D. Mittelstaedt: Preprint.
30. H. L. Reynolds and A. Zucker: Phys Rev. *96*, 393 (1954).

Tryckt den 24 september 1958

Uppsala 1958. Almqvist & Wiksells Boktryckeri AB